nature neuroscience

Salience modulates 20–30 Hz brain activity in *Drosophila*

Bruno van Swinderen & Ralph J Greenspan

Fruit flies selectively orient toward the visual stimuli that are most salient in their environment. We recorded local field potentials (LFPs) from the brains of *Drosophila melanogaster* as they responded to the presentation of visual stimuli. Coupling of salience effects (odor, heat or novelty) to these stimuli modulated LFPs in the 20–30 Hz range by evoking a transient, selective increase. We demonstrated the association of these responses with behavioral tracking and initiated a genetic approach to investigating neural correlates of perception.

The traditional view of the insect brain as limited and inflexible, compared with the vertebrate brain, has given way over the past several decades as research continually reveals unsuspected degrees of sophistication. Honeybees are capable of such complex cognitive functions as associative recall, categorization, contextual learning, allocentric navigational memory and certain forms of abstraction[1]. Fruit flies, although somewhat less versatile, nonetheless show associative learning[2], novelty (incidental) learning[3] and contextual generalization[4]. Central to the performance of these faculties is the ability to assign salience to a stimulus. From observation of behavior alone, however, it is difficult to distinguish an animal's ability to assign salience from its ability to perform the motor task at hand.

Physiological measures of brain events associated with learning in the honeybee[5] and fruit fly[6,7] have focused on the sensory response to olfactory stimuli and inputs to the mushroom bodies, whereas most of the sophisticated cognitive functions of these insects (observed in the laboratory) involve vision[1,3,4]. Recent studies of visual physiology, on the other hand, have been primarily concerned with optic lobe processing of motion detection in the context of the optic flow[8,9]. Little is known of the neural events that occur more centrally in the protocerebrum.

The fruit fly *Drosophila melanogaster* has been used extensively to investigate the relationship between genes and behavior, but has less commonly been used for relating behavior to physiology in the central nervous system. A physiological correlate of the sleep-like state has recently been found in *Drosophila* using a newly developed preparation for recording local field potentials (LFPs)[10]. In the present study, we used this preparation to study the brain responses evoked by visual stimuli and the modulation of these responses in the 20–30 Hz range by salience. Finally, we consider the possible relevance of these findings to a fly's counterpart of selective attention.

RESULTS

Evoked responses

Flies were suspended in the center of a cylindrical arena consisting of green light-emitting diodes (LEDs)[11], and LFP responses to visual stimuli were recorded from their brains (**Fig. 1a**). Animals were not flying, but did very occasionally make spontaneous flight bouts of a few seconds. A visual object (for example, a 10°-wide dark vertical bar on a lit background) was rotated at a constant frequency ('open loop' at 0.33 Hz) for a trial period (200 s). Brain activity was recorded as a voltage differential between an electrode placed in the left optic lobe (lol) and an electrode inserted into the medial protocerebrum (mpc)[10]. The LFP response included large, slow deflections matched exactly to the rotation frequency of the image, as well as faster potentials (>10 Hz) occurring throughout (**Fig. 1b**). A spectral analysis of the brain recording revealed increased power across all frequencies (1–100 Hz; **Fig. 1c**) and increased power at 0.33 Hz (data not shown) when an image was presented. A peak of responsiveness was seen in the 20–30 Hz range (**Fig. 1c**, arrow). Increased 20–30 Hz activity is therefore superimposed on the slow (0.33 Hz) deflections coupled to the rotating image.

The image position–dependence of brain responses (1–100 Hz) was mapped onto the fly's visual field, and the 20–30 Hz range showed the greatest differential between the front and back of the animal (**Fig. 1d**). This partitioning of 20–30 Hz power by image position will be referred to here as the '20–30 Hz response' (calculated as $I = (P - T)/\bar{x}$; see Methods), which is distinct from average 20–30 Hz power ($\bar{x}$). The slower (0.33 Hz) component of the response was also mapped onto the fly's visual field, but by its voltage level instead of power, to reflect its polar character: images sweeping across the left (implanted) eye produced a depolarization in the LFP followed by an equal-sized hyperpolarization after leaving the left visual field (**Fig. 1f**, left). The partitioning of voltage level by image position is termed the 'slow potential response' (Methods).

The slow potential response was very consistent within individual flies, but the 20–30 Hz response varied considerably. The 20–30 Hz response peak for any one fly was found to be very regular with respect to position, yet variable in magnitude from one epoch to the next. **Fig. 1e** (left) shows averaged 20–30 Hz responses to a rotating bar for three successive 1-min epochs, with an inset arrow indicating image rotation direction. The front-to-back difference of the 20–30 Hz signal (that is, the 'response', I) varied up to twofold from minute to minute.

The Neurosciences Institute, 10640 John Jay Hopkins Drive, San Diego, California 92121, USA. Correspondence should be addressed to R.J.G. (greenspan@nsi.edu).

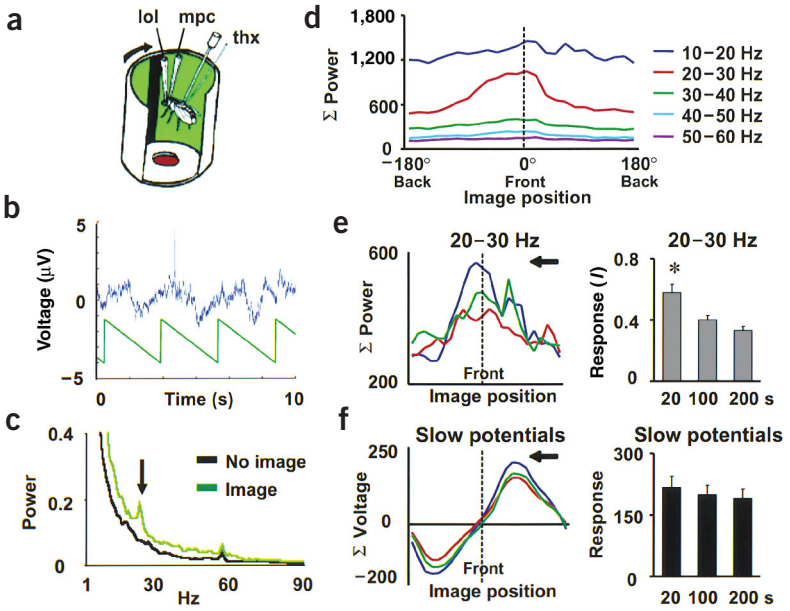

Figure 1 Mapping the LFP signal to image position. (**a**) Setup of experimental arena: a fly was suspended within a programmable visual environment (Methods). Electrodes were implanted into the left optic lobe (lol), medial protocerebrum (mpc) and thorax (thx). (**b**) A sample 10 s of raw brain signal (blue trace) superimposed above the image rotation sequence (green). The angular position of the image is proportional to a voltage signal. (**c**) A sample power spectrum of brain frequencies (1–100 Hz) for a lit but featureless rotating panorama (no image) compared to the spectrum for a lit rotating panorama featuring a 10°-wide unlit vertical bar (image). The arrow points to the 20–30 Hz response to the image. (**d**) A sample 200 s average mapping of the summed (Σ) power of different frequency brackets onto 24 sectors of the panorama. The sector in front of the fly is indicated by a vertical dashed line, corresponding to the 0° position in the visual field. The extremes of the plot correspond to the –180° and 180° positions in the visual field. (In all subsequent figures, the 0° position is represented by the dashed vertical line, labeled 'front'.) (**e**) Successive (blue, red, green) 1-min average 20–30 Hz mappings in a sample fly. Each plot is an average of three 20-s bins. The arrow indicates the image movement direction. Histogram: average 20–30 Hz response data (*I*, response index; Methods) divided into three time bins after initial image presentation ($n = 10$ flies, $^*P < 0.05$ by *t*-test against experimental average). (**f**) Successive 1-min slow potential mappings in the same sample, with corresponding histograms for the slow potential response ($P - T$; Methods).

In contrast, the voltage level of the slow potential was much less variable within individual flies (**Fig. 1f**). Averaged data from ten flies shows that the 20–30 Hz response to an image was significantly greater in the first 20 s of presentation, as compared to the overall experimental average, but this was not the case for the slow potential response (histograms in **Fig. 1e**,**f**).

We further distinguished the 20–30 Hz response from the slow potential response by reversing the direction of image rotation: the 20–30 Hz response peak position was independent of image direction, but the slow potential peak was not. The slow potential's peak positive voltage preceded the average 20–30 Hz response peak for an object rotating clockwise (**Fig. 1e**,**f**; arrow indicates image direction), but followed the 20–30 Hz peak for objects rotating counter-clockwise (not shown). The average peak position of the 20–30 Hz response was similar for both directions (position difference, -0.3 ± 0.47; not significantly different from zero; $n = 10$ flies), whereas the peak of the slow potential differed according to direction of rotation (position difference, 3.6 ± 0.67, $P = 0.0004$, same set). This direction-dependence of the slow potential timing could be accounted for by the fact that the left eye, where the optic lobe electrode was placed, is the first eye stimulated by objects moving clockwise. Objects rotating counter-clockwise have already been 'seen' by the animal before falling directly on the left eye. This suggests a more primary optic-lobe source for the slow potentials and a more processed central source for the 20–30 Hz component of the brain recording. Further localization of the evoked responses, as ascertained by differential recordings to a third electrode in the thorax or with a multichannel electrode in the mpc, indicated an optic-lobe origin for the slow potentials and an mpc origin for the 20–30 Hz response (see results and figure in **Supplementary Note** online).

Attaching salience

Two results presented thus far suggest that the 20–30 Hz evoked response could be a neural correlate of the perceptual event occurring at the onset of object tracking behavior[12]. First, the 20–30 Hz response is greatest upon initial exposure to a rotating image and then can be intermittent throughout the presentation (**Fig. 1e**), as is true of behavioral tracking in flies[12]. Second, the direction-independence of the 20–30 Hz response dissociates it from purely sensory phenomena and implies more of a perceptual role.

To pursue this question, we placed flies in various situations likely to alter stimulus salience. First, we matched the rotation frequency of a bar (0.33 Hz) with a synchronous puff of banana odor within a closed chamber (Methods). We found that adding such a layer of salience increased the 20–30 Hz response to the image specifically, as it also does behaviorally in the flight arena[13]. The response was greatest for the first 20-s epoch following the introduction of the image-matched odor; the magnitude of the response significantly increased, but the peak position did not change (**Fig. 2a**, left). For some flies, this increase persisted, but on average the response returned to pre-salience (baseline) levels after 100 s (**Fig. 2a**, middle). In contrast to the 20–30 Hz response, the slow potential response was not significantly changed by the odor (data not shown). Control experiments using the same set of flies, with the image turned off, showed a phase-matched response to the banana puffs alone, most robust in the 70–80 Hz range, which peaked at a different position than did the image response (**Fig. 2a**, right). Pairing the presentation of image and odor thus increased the 20–30 Hz response to the image specifically at its characteristically mapped position.

When, instead of an odor, short heat-pulses were synchronized to a rotating image (Methods)[14], the 20–30 Hz response showed a similar transient increase from baseline ($P = 0.04$) in the image-appropriate part of the visual field, distinct from the effect of heat pulses alone (0.32 ± 0.05 baseline, 0.46 ± 0.03 for the first 20 s epoch after introducing matched heat pulses, 0.29 ± 0.03 after 100 s; $n = 6$ flies).

We next found that the average 20–30 Hz response to a rotating bar was attenuated during the fly's sleep-like state[15] in overnight

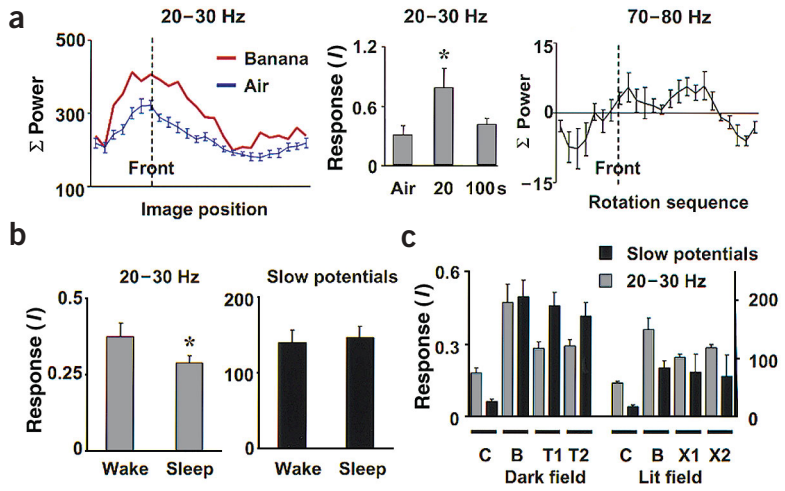

Figure 2 Attaching salience. (**a**) Left, baseline (air) 20–30 Hz response (calculated as *I*; Methods) to the image—a dark bar on a lit background—contrasted with subsequent mapping for the first 20 s epoch of banana odor puffs synchronized to the image rotation in a sample fly. The sector in front of the fly is indicated by a vertical dashed line. Middle, average 20–30 Hz response amplitude (± s.e.m.) at baseline (air) and after 20 s and 100 s of matched odor ($n = 5$ flies; $^*P < 0.05$, *t*-tested against baseline). Right, summed (Σ) power of the 70–80 Hz response to banana alone (without any image) mapped onto the same voltage rotation sequence as the left panel. The plot is an average of normalized summed (Σ) power ± s.e.m. for each sector, with each mean set to zero ($n = 5$ flies). (**b**) Sleep epochs showed a significant decrease in 20–30 Hz response to a rotating bar compared to waking epochs. Slow potentials ($P - T$; Methods) showed no such decrease. Significance was defined by *t*-test comparisons ($P < 0.05$) of combined sleep versus waking averages for all flies ($n = 14$ rest and 14 waking epochs, distributed among 3 flies). (**c**) Different images presented were all rotated clockwise at the same frequency (0.33 Hz). Both brain responses, 20–30 Hz and slow potentials, are shown side-by-side for each image (± s.e.m.). Images in the left group are lit on a dark background and images in the right group are dark on a lit background. All flies were tested for at least two different images (unlit control, $n = 7$; lit control, $n = 13$; bar (B), $n = 14$; upright T (T1) and inverted T (T2), $n = 11$ each; $n = 3$ for each orientation of the × (X1, ×; X2, +)). The Ts and ×s were all equivalent in size, but Ts differed from ×s in luminosity.

experiments (**Fig. 2b**). This attenuated 20–30 Hz response is image-specific and is superimposed on an overall decrease in power found to occur during the sleep-like state[10,16]. In contrast, the slow potentials were unaffected by behavioral state. Thus, the sleep-like state, which has been defined as extended immobility coupled with heightened arousal thresholds in this preparation[10], somehow prevents an intact optic lobe response from achieving salience more centrally.

Third, we found that the magnitude of the (waking) 20–30 Hz response depended on image shape (**Fig. 2c**). In general, vertical bars evoked the greatest 20–30 Hz response compared to other image types. Behaviorally, flies have been shown to respond more to vertical bars than to other image shapes (such as Xs or Ts)[17]. Yet, the 20–30 Hz response to a lit bar on a dark background was not significantly different from the response to a dark bar on a lit background (0.47 ± 0.08 versus 0.36 ± 0.05, $P > 0.05$, $n = 14$ flies). In contrast, the slow potentials did differ significantly between these stimuli: slow potential amplitude differences were larger for the lit bar than for the dark bar (206 ± 29 versus 84 ± 12, $P = 0.00003$). Thus, whereas the responses generated in the optic lobes differed significantly between identical bars of switched luminosity, the 20–30 Hz responses remained similar. Conversely, substituting a 'T' for a bar (lit on dark backgrounds) reduced the 20–30 Hz response (0.29 ± 0.03 versus 0.47 ± 0.08, $P < 0.05$) but not the slow potential response (190 ± 23 versus 206 ± 29, $P > 0.05$, $n = 11$). Thus, the slow potentials are sensitive to luminosity, and the 20–30 Hz response amplitude is sensitive to image shape. Given our previous results, this effect of image shape may reflect the inherent salience of certain images.

Providing choice

We next investigated the relation of the 20–30 Hz response to stimulus selection, defined behaviorally in the flight arena[12,13] where it is manifest in both closed-loop (behavioral feedback) or open-loop (no feedback). In our preparation, the flies are not reporting behaviorally, but rather with an altered 20–30 Hz response to a choice of images (that is, open-loop).

The two images tested, an upright T (T1) and an upside-down T (T2), evoked identical naive responses. When presented separately, yet 180° apart in the image sequence, the two different images map 180° apart onto the rotation sequence (**Fig. 3a**). They each therefore elicit a response commensurate with their position, showing the characteristic increase of the 20–30 Hz response in the first 20 s (**Fig. 3a**, right). Surprisingly, the presentation of both images simultaneously, yet 180° apart, did not produce two response peaks. Rather, the rotating opposing images resulted on average in a flat response, such that no sector of the visual field evoked a greater 20–30 Hz response (**Fig. 3a**). When one of the two images was associated in open loop with heat[14] during a conditioning session, a second simultaneous presentation of both images produced a biased 20–30 Hz response mapping: the average response peak corresponded to the position of the heat-associated image (**Fig. 3b**). This was most pronounced in the first 20-s epoch, with the 20–30 Hz response significantly greater for the heat-associated image of the pair ($P < 0.05$). Heat training to the opposite image produced a corresponding selective response to that object. Thus, the fly's 20–30 Hz response reflects a selective increase in the salience of the trained image and a suppression of response to the non-trained image. Notably, the post-conditioning response peak preceded the naive response peak (previously measured for that image alone) by approximately 450 ms (**Fig. 3a,b**; note that image rotation is represented as right-to-left). This is consistent with the appearance of anticipation or expectancy of the stimulus as a result of conditioning.

Stimulus selection was also observed, albeit less robustly, for novelty conditioning where pre-exposure (training) to one of the two images for 10 min was followed by simultaneous presentation of both. In this protocol, post-training responses mapped closer to the position of the novel image (**Fig. 3c**). This result also mirrors flight arena behavior in a closed loop where, given a choice, flies prefer novelty and can be conditioned by novelty[3].

In addition to position-tagging of multiple images, we explored the generality of the selection effect by using frequency-tagging of simultaneously presented images. The two images were rotated simultaneously but at different frequencies around the fly (0.33 versus 0.66 Hz) and were thus frequency-tagged. The faster image, when presented alone, maps twice for every rotation of the slow image presented alone, when analyzed with the slow-frequency window (**Fig. 3d**, left). When both rotating images were superimposed,

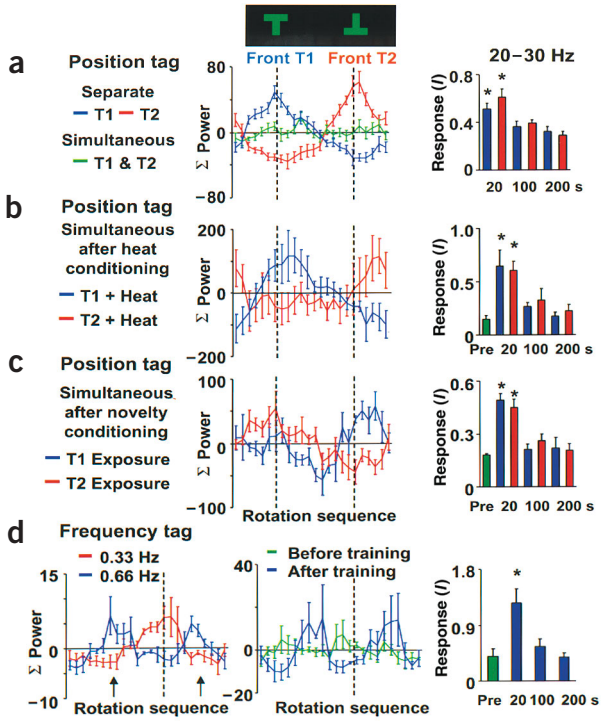

Figure 3 Selective 20–30 Hz response. Two images, an upright and an inverted T of equal proportions and luminosity (top), lit on a dark background, were displayed in opposing sectors of the image rotation sequence such that each image was 'in front' of a fly during a distinct portion of the 360° sequence (vertical dashed lines). (**a**) Average 20–30 Hz mapping for each image presented separately or simultaneously (T1 and T2) for 200-s trials. Each plot is an average of normalized summed (Σ) power (± s.e.m.) for each sector, and for each plot the mean is set to zero ($n = 11$ flies). Right, histograms show the average 20–30 Hz response (I, Methods) for the first 20, 100 and 200 s elapsed for each image presented separately (T1, blue; T2, red). (**b**) Left, the average 20–30 Hz mapping for the first 20-s epoch of simultaneous image presentation after heat conditioning. T1, upright T ($n = 4$ flies); T2, inverted T ($n = 4$ flies, 2 flies in common with T1). Right, the 20–30 Hz response amplitude to the simultaneous image presentation is averaged and plotted for epochs preceding (green) and following the heat conditioning treatment ($n = 4$ trials/treatment). (**c**) The same approach was used for novelty conditioning, except that the conditioning treatment involved exposure to the test image alone, at room temperature, for 10 min. (T1, five flies exposed to an upright T for 10 min; T2, five flies exposed to an inverted T for 10 min (two flies in common with T1). Right, response data were averaged ($n = 5$ trials per treatment) and analyzed as above. (**d**) Frequency tagging. Left, two images (an upright and an inverted T) rotating at different speeds (slow, 0.33 Hz; fast, 0.66 Hz) were presented separately, and the 20–30 Hz mappings were plotted onto a 'slow' analysis window. The fast image was in front twice (arrows) for every rotation that brought the slow image in front (dashed line). Data was normalized and the mean set to zero for averaging ($n = 4$ flies). Middle, both images were presented simultaneously before and after a heat conditioning treatment. The average before-training response and that of the first 20-s after training are shown ($n = 4$ flies). Right, the average response (I) is plotted for the pre-conditioning presentation (green) and three epochs of the post-conditioning presentation of the same stimuli. Significance was determined by t-test against the pre-conditioning baseline response (*$P < 0.05$).

the average 20–30 Hz peak response did not synchronize preferentially to either frequency ('before training' in **Fig. 3d**, middle). In contrast, the same stimuli presented after training sessions, involving heat association to the slower image, synchronized the 20–30 Hz response peak to the faster image alone ('after training'). The response to the slower image was correspondingly suppressed after the heat treatment ($P = 0.004$). Thus, a selective response was extracted from two overlapping images rotating simultaneously at different speeds. That the 20–30 Hz response synchronized to the image not associated with heat was an unexpected result because in the previous experiment (**Fig. 3b**), the response increased selectively for the image that was paired with heat. This suggests the presence of an intrinsic, latent bias brought out by the conditioning paradigm used, but does not detract from the finding that stimulus selection occurred. When, after training, the animals were presented with only the slow image, they responded normally to this otherwise suppressed image (data not shown).

Coherence during selection

Perceptual mechanisms in mammals have been associated with enhanced, temporally correlated neuronal activity[18]. This can be observed as coherence, a measure of the degree of phase locking for particular frequency bands between different parts of the brain. Our multichannel electrode preparations allowed us to measure coherence in the fly brain along a 100-μm vertical axis (**Fig. 4a,b** and **Supplementary Note**). The magnitude of 20–30 Hz coherence correlated well with the fluctuating levels of 20–30 Hz power (average correlation for 200 s of vertical bar presentation, 0.63 ± 0.05; $n = 12$ flies). We then assessed 20–30 Hz coherence changes in flies tested for selective discrimination ($n = 5$ multichannel preparations). In all subjects, 20–30 Hz coherence between brain regions increased significantly in the first 20 s of choice following a training session, and then returned to average baseline levels after the 20-s epoch of increased selection (**Fig. 4c,d**).

Behavioral tracking and the 20–30 Hz response

We then directly tested whether the 20–30 Hz response to salience represents a neural correlate of behavioral tracking in the flight arena[11–13]. Flies implanted with electrodes flew sufficiently well in closed-loop (flight bouts lasted from 10 s to 2 min) to achieve behavioral tracking of an image in the flight arena[11]. During ongoing bouts of flight, transitions from no tracking to tracking were accompanied by significantly increased 20–30 Hz brain activity (1.54 ± 0.11 fold increase, $P = 0.0004$, $n = 3$ transitions in each of four flies, **Fig. 5**). The increased 20–30 Hz activity was mostly transient and generally did not persist throughout continued behavioral tracking. This makes it unlikely that the increased 20–30 Hz activity is an artifact of flight dynamics peculiar to tracking. The association between a behavioral transition to tracking and increased 20–30 Hz brain activity further strengthens the association between the 20–30 Hz response fluctuations in flightless open-loop experiments and behavioral selection.

Genetic dissection of the evoked responses

To delve into mechanisms and brain structures that subserve the 20–30 Hz response, we tested fly strains carrying temperature-sensitive mutations affecting action potentials or synaptic release; some of these strains have mutations that are targeted to specific parts of the nervous system. The mutations' reversibility allowed us to ascertain a baseline response at the permissive temperature (22 °C), a response at the non-permissive temperature (38 °C) and a recovery response following return to the permissive temperature. For each strain, heat-induced deviations from baseline were

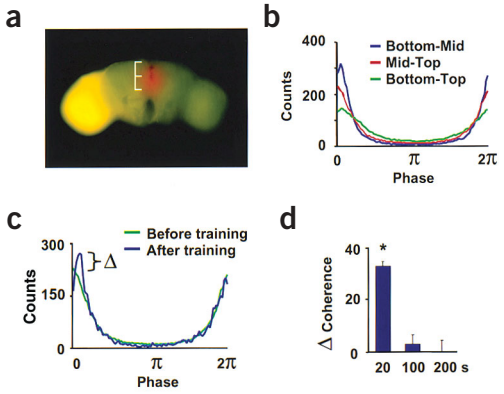

Figure 4 20–30 Hz coherence. (**a**) Each multichannel recording comprises three probes 50 μm apart (inset bar) on a vertical shaft inserted down through the fly's ocelli, parallel to the back of the fly's head, such that the deepest (bottom) is 125–150 μm down from the top of the head. Diffuse red staining is Evan's Blue dye iontophoresed[10] at the depth corresponding to glass electrode and middle multichannel recording positions. (Autofluorescence in the left optic lobe was a consequence of puncturing the left retina during insertion of the optic lobe electrode.) (**b**) An average coherence plot for all three channel combinations in an unconditioned fly. Coherence between channels is represented by the frequency (counts) of fifty 20–30 Hz phase components (abscissa, from 0 to 2π), with synchrony showing a U-shaped curve. (**c**) Baseline mid-top 20–30 Hz coherence (green line) is plotted against the phase counts calculated for the first 20 s epoch following the heat-conditioning treatment (blue line) in one of the stimulus selection experiments. The difference between maxima in both phase plots is indicated by Δ. (**d**) Coherence change (Δ) was calculated as deviations from baseline for three epochs of the post-conditioning period (20, 100 and 200 s). Δ Coherence measurements from different flies were combined and significance was determined by *t*-test against zero ($n = 5$ flies). Bottom-top results are shown; mid-top coherence was also significantly increased ($P < 0.05$), but bottom-mid coherence was not.

calculated (as ratios) for both the 20–30 Hz response (Δ) and for the average 20–30 Hz power ($\bar{x}$) separately. Deviations from the baseline response were also measured for the slow potentials coming from the optic lobe. Complementary experiments in a closed-loop flight arena provided a behavioral test for tracking[12].

We first addressed the source of the slow potentials, the primary visual input, by targeting a temperature-sensitive *shibire* mutation (shi^{ts1})[19,20] to the fly retina. The shi^{ts1} mutant encodes a thermolabile form of the dynamin protein involved in synaptic vesicle recycling, which blocks synaptic transmission at high temperature. Targeting to the retina was achieved with a promoter expressed in most of the photoreceptors[21] in transgenic *Rh1-GAL4/UAS-shi*^{ts1} animals. The slow potential was significantly attenuated in transgenic flies at the restrictive temperature (summed voltage response deviation from baseline, 0.49 ± 0.06; $P = 0.003$, $n = 4$ flies), as was the 20–30 Hz response (Δ ratio, 0.68 ± 0.08; $P = 0.03$, same set). This result is consistent with an optic-lobe localization of the slow potentials and showed that the more central potentials are dependent upon retinal input, as expected[22]. *Rh1-GAL4/UAS-shi*^{ts1} proved to be the only strain (of ten strains tested) in which the slow potential response was significantly affected.

We now focus on the 20–30 Hz response (**Fig. 6**). In wild-type Canton-S (CS) flies, the 20–30 Hz response remained robust (=) during heat (Δ ratio, 1.55 ± 0.49) and recovery (Δ ratio, 1.28 ± 0.14) conditions (**Fig. 6**, top row, second column). Their average 20–30 Hz power was also not affected during heat ($\bar{x}$ ratio = 0.99 ± 0.03), and heated CS flies still responded behaviorally to a vertical bar under closed-loop flight by tracking, albeit less robustly than without heat (**Fig. 6**, columns three and four).

para^{ts1} flies (**Fig. 6**, second row), carrying a mutation that reduces the number of voltage-sensitive sodium channels[23], are paralyzed at 32 °C and hence cannot be tested behaviorally in a flight arena while heated. These immobile (heated) *para*^{ts1} animals still maintained a robust front-to-back 20–30 Hz response (Δ ratio, 1.57 ± 0.13), even while the average 20–30 Hz power, as well as power for all frequencies examined, was significantly attenuated during heat treatment ($\bar{x}$ ratio, 0.61 ± 0.07, $P = 0.01$). Average power returned quickly to baseline as soon as the heat was turned off.

The *Syntaxin1A* mutant *Syx1A*$^{3\text{-}69}$ (**Fig. 6**, third row) is paralyzed at 38 °C by the impairment of synaptic release[24]. Like *para*^{ts1}, these mutants show an overall decrease in the average amount of 20–30 Hz power during heat ($\bar{x}$ ratio = 0.75 ± 0.04, $P = 0.004$), and they also recovered quickly after heat. In contrast to *para*^{ts1}, however, they lost the 20–30 Hz response to a rotating image (Δ ratio, 0.65 ± 0.07, $P = 0.0006$). These findings suggest that action potentials and synaptic potentials, although functionally inter-dependent, may contribute unequally to the 20–30 Hz response. One possibility is that the intact 20–30 Hz response in *para*^{ts1} animals may be a function of local circuits using electrotonic conduction, which does not rely upon action potentials. Alternatively, there could be residual activity in some *para*^{ts1} neurons due to differential sensitivity to the overall reduction in sodium channel number[23].

MJ85b/UAS-shi^{ts1} (**Fig. 6**, fourth row) expresses the thermolabile dynamin protein throughout most, but not all, of the *Drosophila* brain[25]. The animal is thus paralyzed by heat. Although the 20–30 Hz response was attenuated in this strain, the time required to attenuate the response was slower than *Syx1A*$^{3\text{-}69}$ and of variable latency: a sig-

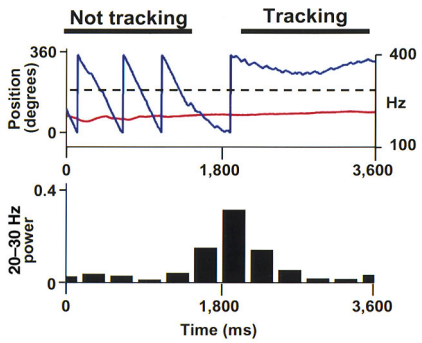

Figure 5 Behavioral tracking and 20–30 Hz brain activity. A sample transition to behavioral tracking during a closed-loop flight bout is shown. The upper panel plots the image position (blue line) through time, where one ratchet represents a 360° rotation (no tracking). The image is in front of the fly at the level of the horizontal dashed line. The red line plots the wing beat frequency of the fly, demonstrating constant flight. The transition period corresponding to the onset of behavioral tracking is represented by the gap between the lines at the top of the figure. The histogram in the lower panel plots average 20–30 Hz power calculated for the same epoch as the behavioral data. Average 20–30 Hz power was determined for the 3-s epochs preceding and following a clean transition to tracking during a flight bout, and a ratio calculated (three transitions per fly, all data averaged and *t*-tested against 1). Only transitions from no tracking ($I = 0$) were considered.

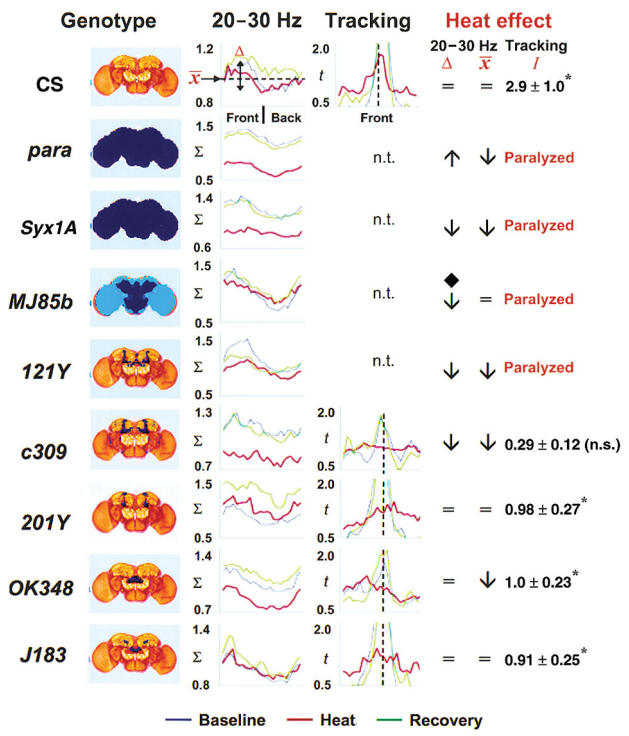

Figure 6 20–30 Hz activity and tracking behavior in mutant strains. Brain localization of genetic lesions (blue) for each fly strain are shown in the first column (*para*^{ts1} and *Syx1A*$^{3\text{-}69}$ are mutations expressed throughout the CNS). Each *GAL4* strain was tested in trans with *UAS-shi*^{ts1}. Summed 20–30 Hz power (Σ) was mapped onto the visual field for three 100-s epochs of open-loop image presentation (second column): baseline at 25° (blue), heat at 38° (red) and recovery at 25° (green). The plots, shifted left to better exemplify peaks and troughs in 20–30 Hz activity, are averages of normalized sector data (in units of 20–30 Hz power) from all flies tested within a genotype. Third column, average tracking behavior under closed-loop conditions without electrodes (colors indicate temperature as above; $n = 6$ flies per genotype) calculated from single flights normalized for length (epochs lasting 50–100 s were used). The traces plot relative time (t) versus image position in the 360° visual field, where t is the average time spent in each of the 24 sectors of 15° each. The front of the fly is indicated with a vertical dashed line. Heat-paralyzed genotypes are not testable (n.t.) behaviorally. Right column, average heat effects on 20–30 Hz activity for both the response (Δ) and the mean ($\bar{x}$) as ratios (over baseline): ↑, increase from baseline; ↓, decrease from baseline; =, no change from baseline (t-tested for significance against 1; $n = 6$ for *para*^{ts1} and *Syx1A*$^{3\text{-}69}$; $n = 4$ for all other strains). For *MJ58b*, diamond in the Δ column indicates that the decrease from baseline took longer to develop than the standard 100-s interval seen for all other genotypes in this figure, and also persisted for longer after heat was turned off (see Results). The corresponding tracking behavior for each genotype during the heated epoch was scored by calculating the tracking index (I) (*$P < 0.05$; n.s., not different from zero). Control strains *UAS-shi*^{ts1}/CS and *c309*/CS each showed a significant tracking response during heat ($I = 1.7 \pm 0.6$ and 1.1 ± 0.2, respectively; data not shown).

nificant reduction was not achieved during 100 s of heat (Δ ratio, 0.79 ± 0.13, $P = 0.16$), but once it was attained, a significant reduction of the 20–30 Hz response persisted for another 100 s after the heat was turned off (Δ ratio, 0.71 ± 0.005, $P = 0.01$). These results resemble the paralytic behavior of flies entirely mutant for *shi*^{ts1}, which exhibit a slow entry into paralysis and a slow recovery[26]. *121Y/UAS-shi*^{ts1} flies (**Fig. 6**, fifth row) express the mutant dynamin protein in the mushroom bodies, central complex and pars intercerebralis of the *Drosophila* brain[27]. Although more restricted than the widely-expressed *MJ85b*, this combination of affected neurons still produced paralysis and rapid loss of the 20–30 Hz response (Δ ratio, 0.66 ± 0.19, $P = 0.02$). The more rapid loss with the limited expression pattern of *121Y*, compared with the much slower kinetics in the widespread expression pattern of *MJ85b*, suggests that the 20–30 Hz response is particularly sensitive to a gross imbalance between brain regions.

As many of the *GAL4/UAS-shi*^{ts1} strains expressing mutant dynamin in the mpc are not paralyzed and can fly even while compromised by heat, we determined whether there was a correspondence between the presence of the 20–30 Hz response and the ability to track a vertical bar in flight. *c309/UAS-shi*^{ts1} flies (**Fig. 6**, sixth row) that express the transgene primarily and extensively in the mushroom bodies[28] fail to respond behaviorally to a bar while flying robustly at the restrictive temperature. Electrophysiological analysis revealed a decrease in 20–30 Hz response (Δ ratio, 0.48 ± 0.13, $P = 0.03$) as well as a decrease in average power in these mutants ($\bar{x}$ ratio, 0.76 ± 0.04, $P = 0.03$). The quick recovery of their brain signal upon returning to the permissive temperature mirrored the quick (~5 s) recovery of their behavioral tracking in the flight arena after heat was turned off.

Three other *GAL4/UAS-shi*^{ts1} combinations (**Fig. 6**, rows 7–9) were also non-paralytic and able to fly at the restrictive temperature, but unlike *c309*, they were still able to track a bar in the flight arena while heated. Their tracking behavior was significantly non-random, but not fully wild-type: although they held the bar consistently in different parts of the visual field, it was not always in front. All three strains (*201Y*, *OK348* and *J183*)[29] also showed 20–30 Hz responses that were not significantly changed by heat (Δ ratios, 1.27 ± 0.15, 0.98 ± 0.11 and 0.78 ± 0.14, respectively). *OK348*, which expresses *shi*^{ts1} mainly in the fan-shaped body of the central complex, showed a moderate attenuation in average 20–30 Hz power during heat ($\bar{x}$ ratio, 0.81 ± 0.02, $P = 0.01$) without compromising the front-to-back difference, indicating that average power *per se* is not critical for the behavioral response. *J183*, which expresses only in a subset of the fan-shaped body as well as in the superior arch, displayed unchanged 20–30 Hz activity as well as retaining the ability to track behaviorally.

The contrast between *201Y* and *c309* is instructive. Both strains show broad expression in γ-lobes of the mushroom bodies, but *c309* also shows extensive expression in α- and β-lobes (as well as scattered expression outside of the mushroom bodies), whereas *201Y* is expressed in only a subset of cells in the α- and β-lobes[28]. Heated *201Y/UAS-shi*^{ts1} animals retained the ability to track behaviorally and showed normal 20–30 Hz brain activity, whereas *c309/UAS-shi*^{ts1} animals did not retain either of these characteristics. These results suggest that the output of a subset of neurons in the mushroom body are required for both the tracking response and for the 20–30 Hz response.

DISCUSSION

We have identified a physiological signature of object salience in the brain of *Drosophila* and have initiated the identification of the networks that subserve it. Although behavioral observation was needed to identify this neural correlate initially, our preparation allows for a physiological measure of salience and subsequent genetic analysis that do not require behavior. Many neurological mutants do not fly readily and some are paralyzed under certain conditions, yet behavioral deficits do not necessarily imply perceptual deficits.

The 20–30 Hz response that we have identified in the fruit fly brain is modulated by salience and correlated with transitions to behavioral

tracking. Thus, we infer that it is centrally involved with perceptual events rather than distal sensory events. The mushroom bodies' role in memory formation and retrieval[2] suggests a basis for the 20–30 Hz modulation by salience: salience does not exist alone but rather is a marker of change, and memory provides a mechanism to detect change. Ongoing fluctuations in the 20–30 Hz response amplitude and coherence may reflect ongoing changes in synaptic output from the mushroom bodies. The open-loop conditioning experiments showed that memory can indeed enhance or suppress the 20–30 Hz response to visual stimuli. It is therefore possible that such a mechanism is not unique to conditioning situations, but is ongoing in relation to recent experience in general. This idea is supported by object fixation experiments on the memory mutants *dunce* and *rutabaga*, whose ability to perform selective discrimination is diminished[30]. The mechanisms subserving memory in the mushroom bodies and interacting structures might have an important role in modulating how and when the 20–30 Hz response occurs.

Although the mushroom body is known to be involved in olfactory learning[2], its role in visually driven behavior is less well established. Visual associative conditioning *per se* does not require functional mushroom bodies[31], consistent with the paucity of direct visual system inputs to those structures in *Drosophila*[32]. A more sophisticated and abstract form of visual learning—context generalization—does require mushroom body activity[4]. This is pertinent to our finding that the 20–30 Hz response to salient visual stimuli is a generalizing response, not limited to a single type of stimulus or modality of reinforcement.

Animals with complex nervous systems actively probe different features in their environment and react according to the salience of the selected features. Behavioral evidence for selective stimulus discrimination has been found in the free flight of the hoverfly *Syritta pipiens*[33], as well as in walking[34] and tethered flight of the fruit fly[12,13], where it has been referred to as selective attention[12]. Whether or not these behaviors correspond to true attentional processes is unresolved, partly because attention has been typically intertwined with consciousness[35–37], the presence of which is moot with respect to animals such as insects. Attempts to establish animal models of attention, however, have provided behavioral criteria for its evaluation[38]: orienting, expectancy, stimulus differentiation (consisting of stimulus salience, discrimination of a critical stimulus from its context and selection among stimuli), sustainability and parallel processing. Of these five criteria, insects clearly meet the first four in flight arena tests for object selection. *Drosophila* flies alternate their fixation between different objects in closed-loop flight paradigms[12,13,30], the differential salience of which can be modulated by an aversive stimulus[13,14]. The 20–30 Hz response reported here represents a physiological correlate of this behavioral stimulus differentiation. It is evoked when a moving image is in front of the fly, it is modulated by image type, it is selective, it is increased by novelty and odor-evoked salience, it is anticipatory, and it is reduced when the fly is in a sleep-like state. In marked contrast, the corresponding optic lobe signal remains unaffected. Whether the 20–30 Hz fluctuations are a cause or a consequence of the change in behavior is unresolved. Clearly, however, overt behavioral tracking is not required for the response.

The fruit fly's LFP responses in the 20–30 Hz frequency range presented here share several key features with physiological correlates in the 40–60 Hz range[39] of selective attention in monkeys and humans. For example, amplitude increases with salience[40], salience can be increased either by an unconditioned stimulus or by novelty[41], selection suppresses the response to simultaneous unattended stimuli, and coherence increases with selective attention[18]. Despite the fruit fly's lack of neuroanatomical homology with primates, our findings indicate that *Drosophila* may have analogous mechanisms of establishing salience and directing selective attention to its world, but a better understanding of how the fly brain actually assigns salience is first required. The identification of a physiological signature of salience in the fruit fly opens up these issues to the power and versatility of genetic analysis.

METHODS

For further detailed methods, see **Supplementary Note** online.

Setup. Flight arena design[11], strains, recording setup[10] (with glass or multichannel silicon electrodes; Center for Neural Communication Technology, University of Michigan) and heat delivery[10,14] were used as described previously. Briefly, a fly was suspended from its dorsal thorax in the center of the arena, surrounded by a programmable visual environment (64 × 24 green LEDs)[11] such as a dark vertical bar moving clockwise (as in **Fig. 1a**). A 45° opening behind the fly allowed for continuous video monitoring. Two electrodes were implanted by stereotaxis into the fly's head[10], one electrode 50–100 μm into the left optic lobe (lol) and the other inserted 75–100 μm into the medial protocerebrum (mpc). A third electrode inserted into the thorax (thx) served both as a ground and as a fly movement detector[10]. The fly's temperature was raised in experiments with conditional mutations by an infra-red beam controlled by a shutter underneath the fly.

Analysis and controls. Channels were sampled[10] and power calculated and plotted for a 180° image rotation window moving in 15° increments over a 20-s window (~6 rotations) in a visual field of 24 overlapping sectors. Peak (P) and trough (T) are defined as the sectors with the greatest and lowest average values, respectively. Mean ($\bar{x}$) is the average for all 24 sectors; the 20–30 Hz response index was calculated as $I = (P - T)/\bar{x}$ for the summed 20–30 Hz power for each sector; the slow potential response ($P - T$) was calculated from mapping of the summed voltage signal onto the 24 sectors. Rotating the fly 90° in the arena correspondingly shifted the position (timing) of both slow-potential and 20–30 Hz responses. Both mapping responses persisted despite changes in image rotation frequency (0.1–1 Hz), image size or luminance. Static images appearing in front of the fly also evoked increased 20–30 Hz power transiently, as compared to unchanging epochs ($P = 0.02$, $n = 4$ flies). 20–30 Hz and slow potential responses decreased to baseline for uniformly lit or dark rotating fields, for rotating images dimmed to darkness, as well as for freshly killed flies, thus excluding apparatus artifacts. Movement artifacts were excluded by constant video and thoracic electrode[10] monitoring.

Behavioral tracking. Behavioral tracking, maintaining an image consistently in any part of the visual field, was monitored in the flight arena[11], quantified as a tracking index (I) analogous to the response index above, from 50–100 s flight bouts) and t-tested against 0. Heat delivery[10] was calibrated to 38 °C by paralysis of $Syx1A^{3\text{-}69}$ flies and by a thermocouple in a fly.

Sleep. Flies were continuously exposed to a lit vertical bar rotating clockwise at 0.33 Hz for 12–15 h overnight in a humidified dark environment. Movement was monitored by the thorax electrode[10]. Average 20–30 Hz responses and average slow potentials were contrasted between sleep epochs (5 min or longer without any detectable movements[10,15]) and waking epochs (5 min immediately following sleep).

Odor and heat pulses. Air was alternately bubbled through either water or imitation banana extract diluted 1:500 in water and streamed through a closed transparent cylindrical chamber containing the fly[11]. Baseline: the response to air with a dark rotating bar. Odor: 1 s of banana odor alternated with 2 s of air for every 3 s of image rotation, with the odor peak coming after the bar had passed in front of the fly. Control: the same alternating air/odor sequence presented in the dark. Heat: a 1-s heat pulse[10] was given for every 3 s of image rotation, coming after the bar had passed in front of the fly. Control: the same alternating heat/non-heat sequence presented in the dark.

Conditioning. Heat conditioning: an upright T and an inverted T placed 180° apart were alternately rotated for 1-min periods (total of 10 min). Continuous

heat (38 °C) was applied to the fly during the presentations of one image and responses were contrasted for simultaneous presentation of both images before and immediately after conditioning. Novelty conditioning: initial exposure to one rotating image for 10 min was followed by simultaneous presentation of both images. Differential responses to simultaneous image presentations were assessed by *t*-tests on four sectors defining the response peak position before and after conditioning.

Frequency tagging. Upright and inverted Ts were rotated clockwise at 0.33 Hz and 0.66 Hz. To establish their 20–30 Hz mapping position at 0.33 Hz, they were displayed separately, and to establish the naive response, they were displayed together. Using spectral analyses of FFT length = 100, differential responses to simultaneous image presentations were assessed as above after heat conditioning.

Coherence. Pairs of signals were bandpass-filtered for 20–30 Hz, the phase between them was calculated for 20-s epochs (total of 200 s) after Hilbert transformation of each[42], and these results were plotted as average histograms of phase counts between 0 and 2π. Coherence magnitude was calculated as the difference between the highest and lowest phase counts and *t*-tested against baseline coherence levels set at 1.

Note: Supplementary information is available on the Nature Neuroscience website.

ACKNOWLEDGMENTS

We thank J. Wagner for technical assistance, E. Izhikevich, Y. Chen and D. Nitz for discussions, and R. Andretic, H. Dierick and J. Gally for comments on the manuscript. Multichannel silicon probes were provided by the U. Michigan Center for Neural Communication Technology and sponsored by NIH NCRR grant P41-RR09754. This work was supported by the Neurosciences Research Foundation.

COMPETING INTERESTS STATEMENT

The authors declare that they have no competing financial interests.

Received 3 February; accepted 2 April 2003
Published online 28 April 2003; doi:10.1038/nn1054

1. Menzel, R. & Giurfa, M. Cognitive architecture of a mini-brain: the honeybee. *Trends Cogn. Sci.* **5**, 62 (2001).
2. Wadell, S. & Quinn, W.G. Flies, genes and learning. *Annu. Rev. Neurosci.* **24**, 1283 (2001).
3. Dill, M. & Heisenberg, M. Visual pattern memory without shape recognition. *Phil. Trans. R. Soc. Lond. B. Biol. Sci.* **349**, 143–152 (1994).
4. Liu, L., Wolf, R., Ernst, R. & Heisenberg, M. Context generalization in *Drosophila* visual learning requires the mushroom bodies. *Nature* **400**, 753 (2001).
5. Menzel, R. Searching for the memory trace in a mini-brain, the honeybee. *Learn. Mem.* **8**, 53 (2001).
6. Wang, Y. *et al.* Genetic manipulation of the odor-evoked distributed neural activity in the *Drosophila* mushroom body. *Neuron* **29**, 267 (2001).
7. Fiala, A. *et al.* Genetically expressed cameleon in *Drosophila melanogaster* is used to visualize olfactory information in projection neurons. *Curr. Biol.* **12**, 1877 (2002).
8. Borst, A. & Haag, J. Neural networks in the cockpit of the fly. *J. Comp. Physiol. A* **188**, 419 (2002).
9. Egelhaaf, M. *et al.* Neural encoding of behaviourally relevant visual-motion information in the fly. *Trends Neurosci.* **25**, 96 (2002).
10. Nitz, D.A., van Swinderen, B., Tononi, G. & Greenspan, R.J., Electrophysiological correlates of rest and activity in *Drosophila melanogaster*. *Curr. Biol.* **12**, 1934 (2002).
11. Lehmann, F. & Dickinson, M.H. The changes in power requirements and muscle efficiency during elevated force production in the fruit fly *Drosophila melanogaster*. *J. Exp. Biol.* **200**, 1133 (1997).
12. Wolf, R. & Heisenberg, M. On the fine structure of yaw torque in visual flight orientation of *Drosophila melanogaster*. II. A temporally and spatially variable weighting function for the visual field. *J. Comp. Physiol. A* **140**, 69 (1980).
13. Guo, A. & Goetz, K.G. Association of visual objects and olfactory cues in *Drosophila*. *Learn. Mem.* **4**, 192 (1997).
14. Wolf, R. & Heisenberg, M. Basic organization of operant behavior as revealed in *Drosophila* flight orientation. *J. Comp. Physiol. A* **169**, 699 (1991).
15. Shaw, J., Cirelli, C., Greenspan, R.J. & Tononi, G. Correlates of sleep and waking in *Drosophila melanogaster*. *Science* **287**, 1834 (2000).
16. Kaiser, W. & Steiner-Kaiser, J. Neuronal correlates of sleep, wakingness and arousal in a diurnal insect. *Nature* **301**, 707 (1983).
17. Mimura, K. Discrimination of some visual patterns in *Drosophila melanogaster*. *J. Comp. Physiol.* **146**, 229 (1982).
18. Niebur, E., Hsiao, S.S. & Johnson, K.O. Synchrony: a neuronal mechanism for attentional selection? *Curr. Opin. Neurobiol.* **12**, 190 (2002).
19. Chen, M.S. *et al.* Multiple forms of dynamin are encoded by *shibire*, a *Drosophila* gene involved in endocytosis. *Nature* **351,** 583 (1991).
20. Kitamoto, T. Conditional modification of behavior in *Drosophila* by targeted expression of a temperature-sensitive *shibire* allele in defined neurons. *J. Neurobiol.* **47**, 81 (2001).
21. Hardie, R.C. *et al.* Calcium influx via TRP channels is required to maintain PIP2 levels in *Drosophila* photoreceptors. *Neuron* **30**, 149 (2001).
22. Keller, A. *et al.* Targeted expression of tetanus neurotoxin interferes with behavioral responses to sensory input in *Drosophila*. *J. Neurobiol.* **50**, 221 (2002).
23. Loughney, K., Kreber, R. & Ganetzky, B. Molecular analysis of the *para* locus, a sodium channel gene in *Drosophila*. *Cell* **58**, 1143 (1989).
24. Littleton, J.T. *et al.* Temperature-sensitive paralytic mutations demonstrate that synaptic exocytosis requires SNARE complex assembly and disassembly. *Neuron* **21**, 401 (1998).
25. Joiner, M.A. & Griffith, L.C. CaM kinase II and visual input modulate memory formation in the neuronal circuit controlling courtship conditioning. *J. Neurosci.* **17**, 9384–9391 (1997).
26. Kim, Y.T. & Wu, C.F. Allelic interactions at the shibire locus of *Drosophila*: effects on behavior. *J. Neurogenet.* **7**, 1–14 (1990).
27. Gatti, S., Ferveur, J.F. & Martin, J.R., Genetic identification of neurons controlling a sexually dimorphic behaviour. *Curr. Biol.* **10**, 667 (2000).
28. Connolly, J.B. *et al.* Associative learning disrupted by impaired Gs signaling in *Drosophila* mushroom bodies. *Science* **274**, 2104 (1996).
29. Joiner, M.A. & Griffith, L.C. Mapping of the anatomical circuit of CaM kinase-dependent courtship conditioning in Drosophila. *Learn. Mem.* **6**, 177 (1999).
30. Wu, Z., Gong, Z., Feng, C. & Guo, A. An emergent mechanism of selective visual attention in *Drosophila*. *Biol. Cyber.* **82**, 61 (2000).
31. Wolf, R. *et al. Drosophila* mushroom bodies are dispensable for visual, tactile and motor learning. *Learn. Mem.* **5**, 166 (1998).
32. Strausfeld, N.J. *et al.* Evolution, discovery and interpetations of arthropod mushroom bodies. *Learn. Mem.* **5**, 11 (1998).
33. Collett, T.S. Some operating rules for the optomotor system of a hoverfly during voluntary flight. *J. Comp. Physiol. A* **138**, 271 (1980).
34. Goetz, K.G. Exploratory strategies in *Drosophila*. in *Neural Basis of Behavioural Adaptations* (eds. Schildberger, K. & Elsner, N.) 47–59 (International Symposium, Tutzing, Germany, 1994).
35. James, W. *The Principles of Psychology* (Henry Holt & Co., New York, 1890).
36. Edelman, G.M. *The Remembered Present* (Basic Books, New York, 1989).
37. Crick, F.H.C. & Koch, C. Towards a neurobiological theory of consciousness. *Semin. Neurosci.* **2**, 263 (1990).
38. Bushnell, P.J. Behavioral approaches to the assessment of attention in animals. *Psychopharmacology (Berl.)* **138**, 231 (1998).
39. Engel, A.K. & Singer, W. Temporal binding and the neural correlates of sensory awareness. *Trends Cogn. Sci.* **5**, 16 (2001).
40. Hillyard, S.A. & Anllo-Vento, L., Event-related brain potentials in the study of visual selective attention. *Proc. Natl. Acad. Sci. USA* **95**, 781 (1998).
41. Lee, T.S., Yang, C.F., Romero, R.D. & Mumford, D. Neural activity in early visual cortex reflects behavioral experience and higher-order perceptual salience. *Nat. Neurosci.* **5**, 589 (2002).
42. Tass, P. *et al.* Detection of n:m phase locking from noisy data: application to magnetoencephalography. *Phys. Rev. Lett.* **81**, 3291 (1998).